ADVANCES IN ATMOSPHERIC SCIENCES, VOL. 28, NO. 5, 2011, 1049–1055

A GCM-Based Forecasting Model for the Landfall of Tropical Cyclones in China

SUN Jianqi*[1,2] (孙建奇) and Joong Bae AHN[2]

[1] *Nansen-Zhu International Research Centre, Institute of Atmospheric Physics, Chinese Academy of Sciences, Beijing* 100029

[2] *Division of Earth Environmental System, Atmospheric Sciences, Pusan National University, Pusan* 609735*, Korea*

(Received 8 October 2010; revised 7 January 2011)

ABSTRACT

A statistical dynamic model for forecasting Chinese landfall of tropical cyclones (CLTCs) was developed based on the empirical relationship between the observed CLTC variability and the hindcast atmospheric circulations from the Pusan National University coupled general circulation model (PNU-CGCM). In the last 31 years, CLTCs have shown strong year-to-year variability, with a maximum frequency in 1994 and a minimum frequency in 1987. Such features were well forecasted by the model. A cross-validation test showed that the correlation between the observed index and the forecasted CLTC index was high, with a coefficient of 0.71. The relative error percentage (16.3%) and root-mean-square error (1.07) were low. Therefore the coupled model performs well in terms of forecasting CLTCs; the model has potential for dynamic forecasting of landfall of tropical cyclones.

Key words: statistical-dynamical model, cyclone forecast, tropical cyclone, coupled model, cross validation

Citation: Sun, J. Q., and J. B. Ahn, 2011: A GCM-based forecasting model for the landfall of tropical cyclones in China. *Adv. Atmos. Sci.*, **28**(5), 1049–1055, doi: 10.1007/s00376-011-0122-8.

1. Introduction

Tropical cyclones (TCs) are extremely destructive weather phenomena. The strong winds and heavy rainfall that accompany these weather events have resulted in numerous disasters in tropical oceans and their surrounding continents. Thus, TC activities have become an important focus of meteorological research over the last several decades.

Since the 1980s, many studies have been performed to better understand TC occurrences over the tropical western North Pacific. The TCs over the western Pacific show strong interannual variability, which is closely related to several factors such as sea surface temperature (Chen et al., 1998; Duan et al., 1998; Chan, 2000; Yumoto and Matsuura, 2001; Wang and Chan, 2002; Camargo and Sobel, 2005), large-scale atmospheric circulations (Ding and Reiter, 1983; Ritchie and Holland, 1999; Matsuura et al., 2003; Ho et al., 2005; Wang and Fan, 2007; Wang et al., 2007; Zhou and Cui, 2008), and sea ice (Fan, 2007). Drawing on these findings, researchers have used statistical methods and climate models to forecast the seasonal frequency of TCs over the tropical western North Pacific (Chan et al., 1998; Chan et al., 2001; Cheung and Elsberry, 2002; Wang et al., 2006; Lang and Wang, 2008; Fan and Wang, 2009; Wang and Qian, 2010). As a result, much improvement has been seen in forecasting the frequency of TCs over the region.

In contrast to TC activity over the open oceans, landfalls of TCs have the potential to impact the lives of millions of people and to cause major economic losses. Studies of the variability of landfalls of TCs over China have been performed by Zhang and Peng (2003), Liu and Chan (2003), and Fydeyasu et al. (2006). The results of these studies have shown the occurrence of CLTC events to be associated with the East Asian summer monsoon circulation, western Pa-

*Corresponding author: SUN Jianqi, sunjq@mail.iap.ac.cn

cific subtropical high (WPSH), and El Niño–Southern Oscillation (ENSO) events. Based on ENSO-related indices, Liu and Chan (2003) developed a statistical prediction model for landfall of TCs along the South China coast. These studies have provided the scientific basis for continuing CLTC research. In addition to the statistical forecast method, dynamic forecasting has emerged as another promising approach for the TCs' seasonal prediction (Vitart and Stockdale, 2001). This study aimed to determine whether the climate model has the potential to forecast landfall of TCs, especially CLTCs.

This paper is divided into six sections. The datasets and the climate model are introduced in section 2. In section 3, the investigations of CLTC-related atmospheric circulations are presented. The predictability of the CLTC by the Pusan National University coupled general circulation model (PNU-CGCM) is explored further in section 4. Sections 5 and 6 contain the discussion and conclusion, respectively.

2. Data and model

This study utilized the dataset of TC activity archived by the Regional Specialized Meteorological Center's Tokyo Typhoon Center. TCs are generally divided into three classes—tropical depressions, tropical storms, and typhoons—depending on their maximum sustained wind speeds. In the current study, a CLTC is defined as a tropical storm or typhoon that makes landfall over China. Although TC data have been collected since 1951, potential reliability problems may invalidate records collected prior to the satellite era. Thus, investigators focused on the period from 1979–2009. The monthly National Centers for Environmental Prediction-Department of Energy (NCEP-DOE) Reanalysis 2 (R-2) was used to investigate atmospheric circulations associated with CLTCs (Kanamitsu et al., 2002).

The PNU-CGCM is part of the Asia-Pacific Economic Cooperation Climate Center (APCC) multimodel ensemble long-range prediction system. PNU-CGCM v1.0 is a fully coupled ocean–atmosphere-land–sea-ice model. The model consists of the 18-level National Center for Atmospheric Research Community Climate Model (CCM3, T42), the 29-level Geophysical Fluid Dynamics Laboratory Modular Ocean Model (MOM3), and the Los Alamos National Laboratory elastic viscous plastic sea-ice model. The oceanic component of the CGCM–MOM3 has a horizontal resolution of 2.8125° longitude. However, it has a variable grid system in latitude, with finer resolution at equatorial regions (0.7° at latitudes below 30°, 1.4° at latitudes between 30° and 60°, and 2.8° at latitudes above 60°) to resolve tropically trapped ocean waves, which appear to play important roles in tropical ocean dynamics. No type of flux adjustment was applied to the experiments. This ensured that the coupled state focused solely on the initial value problem and that the model determined this state independently.

The PNU-CGCM hindcasts for the July–August–September (JAS) season for the period 1979–2009 [with initial conditions from January (6–9-month lead), April (3–5-month lead), and July (0–2-month lead)] were used to investigate the dynamic prediction ability of the CLTC. For each initial month, the model forecasts were run using five initial conditions: the 1st, 3rd, 5th, 7th, and 9th days of the initial month. Data on initial atmospheric conditions were obtained from R-2. To initialize marine conditions, the OGCM was run for 100 years prior to the years of interest until it reached a quasi-equilibrium state under the observed atmospheric boundary conditions. Because our forecast span was confined to < 1 year, we assumed that a 100-year ocean spin-up period was sufficient for the upper ocean to reach a quasi-equilibrium state. Following this initialization period, the OGCM was further run under the observed atmospheric boundary conditions for the period 1979–2009. These reproduced ocean states were finally used as the initial conditions of the OGCM in the coupled hindcast experiment. The PNU-CGCM JAS hindcasts were based on an ensemble average of the five members (five initial conditions' runs). This analysis revealed that the coupled model exhibited virtually no forecasting ability in predicting 6–9-month and 3–5-month leads for CLTCs. However, the forecasting ability of the model was better in terms of predicting 0–2-month leads. The following analysis therefore analyzes the results from hindcasts with 0–2-month leads.

3. CLTC-related atmospheric circulations

An analysis of the seasonal cycle of CLTCs indicates that, between January and March, no TCs made landfall over China. Beginning in April, the number of CLTCs began to increase and reached a peak during July before decreasing. Although the CLTCs occurred from April to December, $\sim$80% of CLTCs occurred during the 3 months of JAS (Fig. 1). Thus, we focused on this period. The total number of CLTCs in this season is referred to as the CLTC index.

Chan and Gray (1982) reported that the movement of TCs is largely determined by ambient flow at tropospheric middle levels (700 hPa and 500 hPa). Subsequently, Harr and Elsberry (1991, 1995) also demonstrated the important role of the 700-hPa large-scale

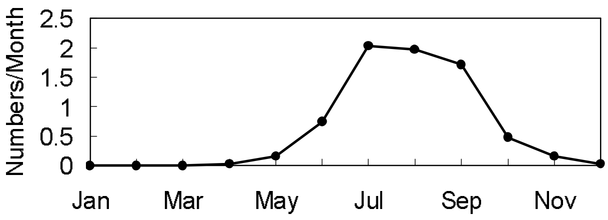

Fig. 1. Annual cycle of the CLTCs over the period from 1979–2009.

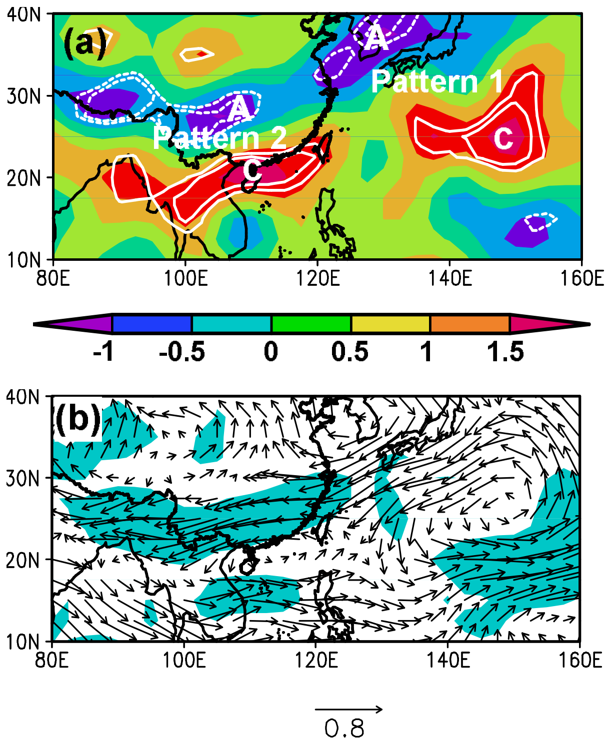

Fig. 2. Regression patterns of (a) 700 hPa vorticity and (b) 700 hPa horizontal winds from R-2 against the observed CLTC index over the period of 1979–2009. "A" ("C") indicates the anomalous anticyclone (cyclone). Solid (dashed) white lines in (a) indicate the positively (negatively) significant areas at the 95% and 98% confidence levels. Shading in (b) indicates the areas at the 95% confidence level.

circulations on the western North Pacific tropical cyclone track. Thus, in the following analysis, CLTC-related circulations over the 700-hPa and 500-hPa levels are emphasized.

Figure 2a presents a regression of the 700-hPa vorticity from R-2 against the CLTC index. The data indicate that there are two significant dipole patterns over the North Pacific–East Asian region. Pattern 1 shows a significant anomalous anticyclone over the Yellow Sea–Korea–Japan and a cyclone south of Japan (Fig. 2), which suggests that the WPSH should be located farther northwest. This point is further confirmed by composite analysis. As shown in Fig. 3, the WPSH shifted farther northwest in years with more CLTCs compared to years with fewer CLTCs. A northwestward shift in WPSH can bring the clockwise airflow on its western flank farther westward, thereby increasing the probability of TCs reaching China but reducing the probability of their making landfall on the Korean Peninsula (Zhang and Peng, 2003; Choi et al., 2009). Pattern 2 shows a strong anomalous cyclone centered over the North India–Indochina Peninsula region and anticyclone over southwestern China (Fig. 2). This meteorological pattern indicates that the Asian summer monsoon trough is enhanced over the western North Pacific. Using the dynamic monsoon index (Wang and Fan, 1999), the correlation coefficient between the monsoon trough and CLTCs was calculated: These two systems are significantly correlated. These analyses indicate that the monsoon trough plays a significant role in the variability of the CLTCs, which is consistent with the findings of previous studies (Harr and Elsberry, 1995; Chu, 2004; Chu et al., 2007). These earlier researches have found that, when an enhanced monsoon trough is present, the equatorial westerly winds and subtropical easterly winds can generate low-level cyclonic shear and cyclonic relative vorticity. In doing so, they create conditions that favor the formation of TCs. Statistical results showed that TCs occurring in the monsoon trough account for 73% of the total number of TCs over the western North Pacific and 79% of the total number of CLTCs (Gao et al., 2008). In addition to affecting the formation of TCs, the southeasterly winds passing over the eastern flank of the monsoon trough can provide a steering flow that enables TCs to reach the Chinese coast. Thus, in a strong monsoon trough year, more TCs occur over the western North Pacific, and more TCs make landfall over China.

At 500 hPa, CLTC-related circulations exhibit a pattern similar to that observed at 700 hPa. We conclude, therefore, that these two dipole patterns provide a favorable background for TCs to make landfall over China.

4. Ability of the PNU-CGCM to predict CLTCs

To investigate the ability of the PNU-CGCM to predict CLTCs, we first explored whether the coupled model could predict the observed relationship between atmospheric circulations and CLTCs.

Figure 4a shows a regression of the 700-hPa vorticity predicted by the PNU-CGCM against the CLTC

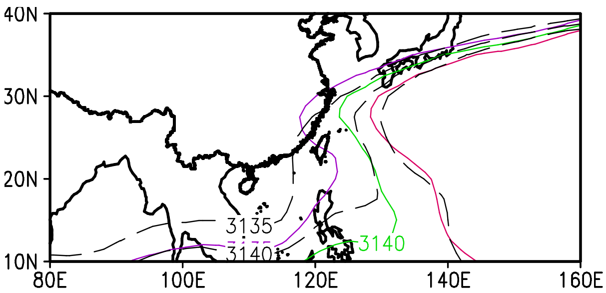

Fig. 3. Composite summer WPSH and Asian monsoon trough at 700 hPa in the years with more (solid line) and fewer (dashed line) CLTCs.

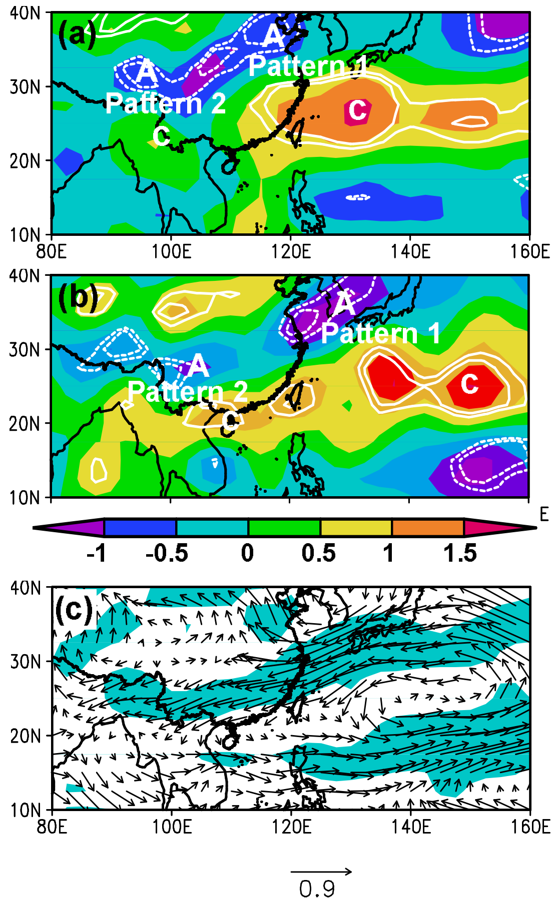

Fig. 4. Regression patterns of (a) 700 hPa vorticity from the PNU-CGCM against the observed CLTC index as well as (b) 700 hPa vorticity and (c) 700 hPa horizontal winds from R-2 against the PNU-CGCM predicted CLTC index over the period of 1979–2009. "A" ("C") in (a) and (b) indicates the anomalous anticyclone (cyclone). Solid (dashed) white lines indicate the positively (negatively) significant areas at the 95% and 98% confidence levels. Shading in (c) indicates the areas at the 95% confidence level.

index. The data suggest that TC-related circulations in the coupled model also show two dipole patterns over the western Pacific–East Asian region that are similar to the observational findings (Fig. 2a). However, in Pattern 2 the activity of the anomalous cyclone in the coupled model is weaker than in the observation, whereas the anomalous cyclone activity of Pattern 1 is stronger. Moreover, compared to the observation data, the positions of the dipole patterns shift eastward in the model.

To address the question of why a spatial shift is simulated for these patterns, we investigated the simulating capability of the PNU-CGCM for East Asian circulations. As shown in Fig. 5, two major atmospheric activity centers occur over the East Asian region during the summer: the WPSH and the Asian summer monsoon trough. These two atmospheric circulations are key factors influencing the CLTCs as discussed in the previous section. A comparison to the observational features (Fig. 5a) shows that the coupled model demonstrates a strong ability to simulate these two atmospheric circulations. However, the simulated WPSH in Fig. 5b is stronger and is located farther west than is shown by the observational data. During such changes in the WPSH, the eastward extension of the Asian summer monsoon trough is confined. In the observation data, the monsoon trough extends as far as 140°E, while in the simulation it only reaches as far as 125°E. Thus, in the PNU-CGCM, the locations of the WPSH and the Asian summer monsoon trough were predicted to occur somewhat farther west than the observation data show. Consequently,

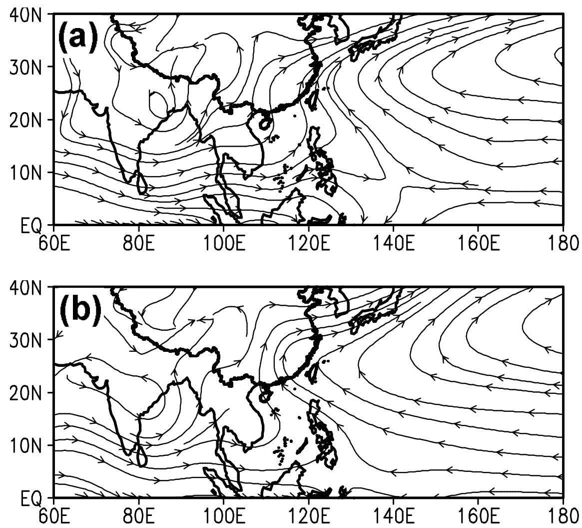

Fig. 5. Climatological distributions of 700 horizontal wind streamline in (a) observation and (b) simulation.

these two atmospheric-circulation-related dipole patterns also shift westward in the coupled model.

Because the anomalous cyclone of Pattern 1 and the anticyclone of Pattern 2 in the coupled model show more significant correlation with the CLTC index, the averaged mean of vorticities over the two circulation centers (Pattern 1: 30°–32.5°N, 92.5°–97.5°E; Pattern 2: 25°–30°N, 127.5°–132.5°E) were selected as indices to represent the two dipole patterns' variability. A statistical dynamic forecast model (SDFM) was then developed based on the multiple linear regression between the two hindcast dipole patterns' indices and the observed CLTC index over the period 1979–2009. The formula of the SDFM is as follows:

$$y = 0.95x_1 - 0.43x_2 + 5.71,$$

where y is the simulated CLTC index, and x_1 and x_2 are the normalized Pattern 1 and Pattern 2 indices, respectively.

Figure 4b and Figure 4c show the regression pattern of the 700-hPa vorticity and horizontal winds from the R-2 against the CLTC index simulated by SDFM. The data show two dipole patterns and their associated circulations to have a quite similar distribution to the observational patterns in Fig. 2, although some visual differences in the magnitude of the values can be seen. The spatial correlation between Fig. 4b and Fig. 2a was 0.88 for 429 samples, which is significant at the 99% confidence level. These findings indicate that the coupled model performs well in terms of simulating the observed spatial–temporal relationship of the CLTC with the two-dipole patterns, even though a spatial shift in position occurred.

Figure 6 presents the observed and simulated CLTC indices for every year during the period 1979–2009. The data suggest that the SDFM was well able to reproduce CLTC variability for the past 31 years. The correlation coefficient between the two indices was 0.77, demonstrating that the coupled model can simulate > 50% of the observed variance in the CLTC index. In the past 31 years, the relative error was 14.7%, and the root-mean-square error (RMSE) was 0.96. To further evaluate the SDFM, a leave-one-out cross-validation analysis was performed. The results suggest that the SDFM has good forecasting capabilities in relation to CLTCs, with a correlation coefficient of 0.71 between the forecasted and observed CLTC indices, a relative error of 16.3% and a RMSE of 1.07.

5. Discussion

Based on five predictors associated with high-latitude circulations in both hemispheres, as well as with circulations over the local, tropical western North Pacific Ocean, Fan (2009) created a statistical prediction scheme for CLTCs. The cross-validation test results of her work show that during 1977–2007 the model accurately predicted CLTCs, with an RMSE value of 1.4 and a correlation coefficient of 0.74. Our results indicate that the CGCM also has a comparable predictive capability for the CLTCs, with a correlation coefficient of 0.71 and an RMSE value of 1.07. One problem with purely statistical forecasting models is that the predictors used in the model are obtained from some preseason climate systems. The indirect impact of these preseason conditions on the predictions could change over time (e.g., Wang, 2002). In contrast to purely statistical forecasting models, SDFMs derive predictors from model-predicted fields, and these predictors directly impact the predicted results. Thus, the predictive capability of the SDFM should remain stable over time. This point is well illustrated in Fig. 7. We also developed four additional forecasting models. The models are based on multiple linear regressions between the indices of the two hindcast dipole patterns and the observed CLTC index, but they utilize different calibration periods: 15 years,

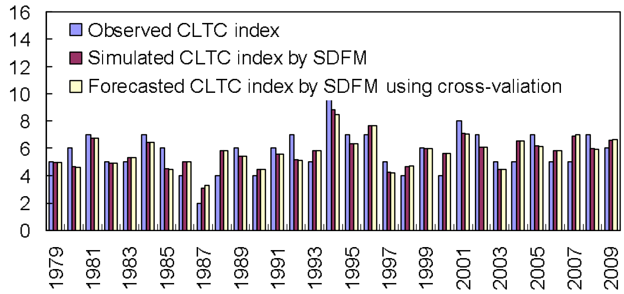

Fig. 6. Time series of the observed CLTC index, simulated CLTC index by the SDFM and the forecasted CLTC index by the SDFM using cross-validation for the 1979–2009 period.

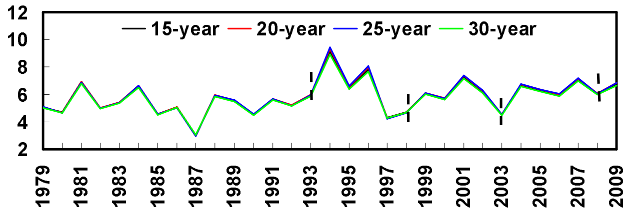

Fig. 7. Time series of the simulated CLTC numbers from the SDFM with 15-year (1979–1993), 20-year (1979–1998), 25-year (1979–2003) and 30-year (1979–2008) calibration periods and the forecasted CLTC numbers over the remaining 16-year (1994–2009), 11-year (1999–2009), 6-year (2004–2009) and 1-year (2009) validation periods.

1979–1993; 20 years, 1979–1998; 25 years, 1979–2003; and 30 years, 1979–2008. Using these four models, we forecast the numbers of CLTCs in the remaining periods: 16 years (1994–2009), 11 years (1999–2009), 6 years (2004–2009), and 1 year (2009). As shown in Fig. 7, the CLTC numbers forecast using these four statistical dynamic models yielded highly consistent results. Even when only the 15-year dataset was used, the model was able to forecast the sudden increase in the CLTC index in 1994 and its downward trend thereafter. The findings show that, unlike the purely statistical forecasting model, the predictive ability of the SDFM is not highly variable over time, thereby demonstrating the model's strong potential for CLTC forecasting.

6. Conclusions

In this study, we explored the ability of the coupled climate model to predict CLTCs by analyzing PNU-CGCM 31-year hindcasts. The results suggest that this coupled model has the ability to predict the relationship between CLTC variability and steering atmospheric circulations reported in observational studies. We also developed a statistical dynamic forecasting model based on multiple linear regressions between the indices of the two hindcast dipole patterns of the PNU-CGCM and the observed CLTC index over the period 1979–2009. An evaluation of the model indicates that the forecasting model has a strong ability to predict CLTC variability, both at year-to-year and decadal time scales. The predictive ability of the forecast model is stable in relation to CLTCs, which to some extent resolves one problem that plagues purely statistical forecasting models, namely that the predicted results may change over time. Therefore, the statistical dynamic model represents a promising approach for predicting landfall of TCs. Only one coupled model was employed in this analysis. Additional studies are needed to investigate hindcasts involving multiple coupled models and to compare the results with those from other models.

Acknowledgements. This work was jointly supported by the Chinese Academy of Sciences key program (Grant No. KZCX2-YW-Q03-3), the Korea Meteorological Administration Research and Development Program (Grant No. CATER 2009-1147), the Korea Rural Development Administration Research and Development Program, and the National Basic Research Program of China (Grant No. 2009CB421406).

REFERENCES

Camargo, S. J., and A. H. Sobel, 2005: Western North Pacific tropical cyclone intensity and ENSO. *J. Climate*, **18**, 2996–3006.

Chan, J. C. L., 2000: Tropical cyclone activity over the western North Pacific associated with El Niño and La Niña events. *J. Climate*, **13**, 2960–2972.

Chan, J. C. L., and W. M. Gray, 1982: Tropical cyclone movement and surrounding flow relationships. *Mon. Wea. Rev.*, **110**, 1354–1374.

Chan, J. C. L., J. E. Shi, and C. M. Lam, 1998: Seasonal forecasting of tropical cyclone activity over the western North Pacific and the South China Sea. *Wea. Forecasting*, **13**, 997–1004.

Chan, J. C. L., J. E. Shi, and K. S. Liu, 2001: Improvements in the seasonal forecasting of tropical cyclone activity over the western North Pacific. *Wea Forecasting*, **16**(4), 491–498.

Chen, T., S. P. Weng, N. Yamazaki, and S. Kiehne, 1998: Interannual variation in the tropical cyclone formation over the western North Pacific. *Mon. Wea. Rev.*, **126**, 1080–1090.

Cheung, K. K., and R. L. Elsberry, 2002: Tropical cyclone formation over western North Pacific in the Navy Operational Global Atmospheric Prediction System forecasts. *Wea. Forecasting*, **17**, 800–820.

Choi, K. S., B. J. Kim, D. W. Kim, and H. R. Byun, 2009: Interdecadal variation of tropical cyclone making landfall over the Korean Peninsula. *Int. J. Climatol.*, doi: 10.1002/joc.1986.

Chu, P. S., 2004: ENSO and tropical cyclone activity. *Hurricanes and Typhoons: Past, Present, and Potential.* R. J. Murnane and K.-B. Liu, Eds., Columbia University Press, 297–332.

Chu, P. S., X. Zhao, C. T. Lee and M. M. Lu, 2007: Climate prediction of tropical cyclone activity in the vicinity of Taiwan using the multivariate least absolute deviation regression method. *Terr. Atmos. Oceanic Sci.*, **18**(4), 805–825.

Ding, Y. H., and E. R. Reiter 1983: Large-scale circulation conditions affecting the typhoon formation over the western Pacific. *Acta Oceanologica Sinica*, **5**, 561–574. (in Chinese)

Duan, Y. H., Z. H. Qin, J. F. Gu, and Y. P. Li, 1998: Numerical study on the effect of sea surface temperature on tropical cyclone intensity. Part I: Numerical experiment of the tropical cyclone intensity related to SST. *Acta Meteorologica Sinica*, **12**, 142–148.

Fan, K., 2007: New predictors and a new prediction model for the typhoon frequency over western North Pacific. *Science in China Series* (*D*), **50**(9), 1417–1423.

Fan, K., 2009: Seasonal forecast model for the number of tropical cyclones to make landfall in China. *Atmos. Oceanic Sci. Lett.*, **2**, 251–254.

Fan, K., and H. J. Wang, 2009: A new approach to forecasting typhoon frequency over the western North Pacific. *Wea. Forecasting*, **24**, 974–986.

Fudeyasu, H., S. Iizuka, and T. Matsuura, 2006: Impact of ENSO on landfall characteristics of tropical cyclones over the western North Pacific during the summer monsoon season. *Geophys. Res. Lett.*, **33**, L21815, doi: 10.1029/2006GL027449.

Gao, J. Y., X. Z. Zhang, Z. H. Jiang, and L. J. You, 2008: Anomalous western North Pacific monsoon trough and tropical cyclone activities. *Acta Oceanologica Sinica*, **30**(3), 35–47. (in Chinese)

Harr, P. A., and R. L. Elsberry, 1991: Tropical cyclone track characteristics as a function of large-scale circulation anomalies. *Mon. Wea. Rev.*, **119**, 1448–1468.

Harr, P. A., and R. L. Elsberry, 1995: Large-scale circulation variability over the tropical western North Pacific. Part I: Spatial patterns and tropical cyclone characteristics. *Mon. Wea. Rev.*, **123**, 1225–1246.

Ho, C. H., J. H. Kim, H. S. Kim, C. H. Siu, and D. Y. Gong, 2005: Possible influence of the Antarctic Oscillation on tropical cyclone activity in the western North Pacific. *J. Geophys. Res.*, **110**, D19104, doi: 10.1029/2005JD005766.

Kanamitsu, M., W. Ebisuzaki, J. Woollen, S. K. Yang, J. J. Hnilo, M. Fiorino, and G. L. Potter, 2002: NCEP-DEO AMIP-II Reanalysis (R-2), *Bull. Amer. Meteor. Soc.*, **83**, 1631–1643.

Lang, X. M., and H. J. Wang, 2008: Can the climate background of western North Pacific typhoon activity be predicted by climate model? *Chinese Science Bulletin*, **53**(15), 2392–2399.

Liu, K. S., and J. C. L. Chan, 2003: Climatological characteristics and seasonal forecasting of tropical cyclones making landfall along the South China coast. *Mon. Wea. Rev.*, **131**, 1650–1662.

Matsuura, T., M. Yumoto, and S. Iizuka, 2003: A mechanism of interdecadal variability of tropical cyclone activity over the western North Pacific. *Climate Dyn.*, **21**, 105–117.

Ritchie, E. A., and G. J. Holland, 1999: Large-scale patterns associated with tropical cyclogenesis in the western Pacific. *Mon. Wea. Rev.*, **127**, 2027–2043.

Vitart, F., and T. N. Stockdale, 2001: Seasonal forecasting of tropical storms using coupled GCM integrations. *Mon. Wea. Rev.*, **129**, 2521–2537.

Wang, B., and J. C. L. Chan, 2002: How does ENSO regulate tropical storm activity over the western North Pacific. *J. Climate*, **15**, 1643–1658.

Wang, B., and Z. Fan, 1999: Choice of South Asian Summer Monsoon Indices. *Bull. Amer. Meteor. Sci.*, **80**, 629–638.

Wang, H. J., 2002: The instability of the East Asian summer monsoon ENSO relations. *Adv. Atmos. Sci.*, **19**, 1–11.

Wang, H. J., and K. Fan, 2007: Relationship between the Antarctic Oscillation and western North Pacific typhoon frequency. *Chinese Science Bulletin*, **52**, 561–565.

Wang, H. J., and Z. L. Qian, 2010: A potential high-score scheme for the prediction of Atlantic storm activity. *Atmos. Oceanic Sci. Lett.*, **3**(2), 1–4.

Wang, H. J., X. M. Lang, K. Fan, J. Q. Sun, and G. Q. Zhou, 2006: Real-time climate prediction experiment for the typhoon frequency in the western North Pacific for 2006. *Climatic and Environmental Research*, **11**(2), 133–137. (in Chinese)

Wang, H. J., J. Q. Sun, and K. Fan, 2007: Relationship between the North Pacific Oscillation and the typhoon/hurricane frequencies. *Science in China*(D), **50**(9), 1409–1416.

Yumoto, M., and T. Matsuura, 2001: Interdecadal variability of tropical cyclone activity in the western North Pacific. *J. Meteor. Soc. Japan*, **79**(1), 23–35.

Zhang, Q. Y., and J. B. Peng, 2003: The interannual and interdecadal variations of East Asian summer circulation and its impact on the landing typhoon frequency over China during summer. *Chinese J. Atmos. Sci.*, **27**, 97–106. (in Chinese)

Zhou, B. T., and X. Cui, 2008: Hadley circulation signal in the tropical cyclone frequency over the western North Pacific. *J. Geophys. Res.*, **113**, D16107, doi: 10.1029/2007JD009156.